

# Possible Coexistence of Superconductivity and Magnetism in Intermetallic NiBi<sub>3</sub>

Esmeralda Lizet Martinez Piñeiro, Brenda Lizette Ruiz Herrera, and Roberto Escudero\*  
*Instituto de Investigaciones en Materiales, Universidad Nacional  
 Autónoma de México. A. Postal 70-360. México, D.F. 04510 MÉXICO.*

Lauro Bucio  
*Instituto de Física, Universidad Nacional Autónoma de México. México, D.F. 04510 MÉXICO.*  
 (Dated: January 13, 2011)

NiBi<sub>3</sub> polycrystals were synthesized via a solid state method. X-ray diffraction analysis shows that the main phase present in the sample corresponds to NiBi<sub>3</sub> in a weight fraction of 96.82 % according to the refinement of the crystalline structure. SEM - EDS and XPS analysis reveal a homogeneous composition of NiBi<sub>3</sub>, without Ni traces. The powder superconducting samples were studied by performing magnetic measurements. The superconducting transition temperature and critical magnetic fields were determined as  $T_C = 4.05$  K,  $H_{C1} = 110$  Oe and  $H_{C2} = 3,620$  Oe. The superconducting parameters were  $\xi_{GL} = 301.5$  Å,  $\lambda_{GL} = 1549$  Å, and  $\kappa = 5.136$ . Isothermal measurements below the transition temperature show an anomalous behavior. Above the superconducting transition the compound presents ferromagnetic characteristics up to 750 K, well above the Ni Curie temperature.

PACS numbers: Intermetallic Alloys; Superconductivity; Ferromagnetism;

## I. INTRODUCTION

The coexistence of superconductivity and magnetism is a phenomena of great interest in the scientific community. In 1957, Ginzburg [1] considered that the coexistence could exist if the critical field were longer than the induction created by the magnetization. Two years before the antagonic nature of superconductivity and magnetism was confirmed when Matthias' experiments [2] showed that the superconductivity in lanthanum was destroyed by a small concentration of magnetic impurities. This was explained as in conventional *s*-wave superconductors, local magnetic moments break up spin singlet cooper pairs and hence strongly suppress superconductivity, an effect known as magnetic pair-breaking. Because of the pair-breaking effect, in most superconductors the presence of only a 1% level of magnetic impurity can result in the almost complete destruction of the superconducting behavior.

The discovery of rare earth ternary and actinide compounds was the first opportunity to study the interaction between the magnetic moments of *f*-electrons and superconducting electrons in a very high density of local moments [3–5]. These compounds presented new exotic phenomena associated with the long-range order of local magnetic moments, such as reentrant superconductivity [6], coexistence of superconductivity and ferroantiferromagnetism [7], magnetic field inducing superconductivity [8] and heavy fermion superconductivity [9].

NiBi<sub>3</sub> is an intermetallic alloy with orthorhombic structure, CaLiSi<sub>2</sub>-type and space group Pnma [10, 11]. In this structure, bismuth atoms form an octahedral array, while nickel atoms form part of linear chains. NiBi<sub>3</sub> is

a superconducting material with a critical temperature about 4.05 K [12], and is the object of study of this research.

Some initial studies has been done on the superconducting properties of NiBi<sub>3</sub>. For instances Fujimori, et al. [13] have presented a study related to the superconducting and normal properties; they studied the resistivity, heat capacity, upper critical magnetic field, in polycrystals and needle like single crystals.

Among the electronic characteristics of this intermetallic alloy is that it presents a large phonon resistivity due to predominant coupling of electrons by bismuth vibrations via the Ni vibrations. In this study we are mainly concerned with the magnetic-superconducting interacting effects, as we will discussed in the rest of the paper.

## II. EXPERIMENTAL DETAILS

Several samples were studied. The preparation method for the most pure obtained sample was the following: the NiBi<sub>3</sub> composition was prepared by solid state method using Bi pieces (Aldrich 99.999 %) and Ni powder (Strem Chemicals 99.9 %) in evacuated quartz tubes. The samples were melted in a resistance furnace at 1000° C for seven days. The characterization was made by X-ray powder diffraction (XRD) (Bruker AXS D8 Advance) using Cu K $\alpha$  radiation, scanning electron microscopy (SEM - EDS) (Leica-Cambridge), and X-ray photoelectron spectroscopy (XPS) (Microtech Multilab ESCA2000) using Al K $\alpha$  radiation 1453.6 eV. The XPS spectra was obtained in the constant pass energy mode (CAE)  $E_0 = 50$  and 20 eV for survey and high resolution respectively. The sample was etched for 20 minutes with Ar<sup>+</sup> at 3.5 kV during 20 minutes at 0.12  $\mu$ A mm<sup>-2</sup>. The peak binding energy (BE) positions were referenced to

---

\* correspondence author: escu@servidor.unam.mx

Au  $4f_{7/2}$  at 84.00 eV and Ag  $3d_{5/2}$  at 367.30 eV having a FWHM of 1.02 eV. Magnetization measurements and determination of the superconducting properties were performed using a Quantum Design (QD) superconducting quantum interference device (SQUID) MPMS system. We determined the transition temperature with magnetization versus temperature  $M(T)$  measurements with a small magnetic field about 10 Oe. Two normal distinct measuring modes were used, zero field cooling (ZFC) and field cooling (FC). Critical magnetic fields were determined by performing isothermal measurements  $M(H)$  at different temperatures, from 2 to 4K. We also performed isothermal measurements at different magnetic intensities at higher temperatures to observe possible magnetic behavior above the transition temperature and at much higher temperatures. In order to determine the Curie temperature and to discard the possibility of Ni as an impurity in the compound, we performed studies to observe in the isothermal curves,  $M-H$ , the existence of hysteresis, thus the coercitive field at different temperatures, and well above the Ni and NiBi Curie temperatures using a Quatum Design oven installed in the MPMS.

### III. RESULTS AND DISCUSSION

#### A. Structural characterization

The structural characterization determined by powder XRD and Rietveld refinement are shown in Fig. 1. The polycrystalline phases were identified by comparison with X-ray patterns in the Inorganic Crystal Structure Database (ICSD) 2010. All the peaks correspond to the  $\text{NiBi}_3$  phase (ICSD 58821), except the weak peaks related to impurities of Bi (ICSD 64703) and NiBi (ICSD 107493), in a proportion less than 1 and 2 % respectively. According to the results of the refinement, no Ni impurities were detected.

Refinement of the crystalline structure was performed using a Rietveld Fullprof program. Table 1 contains the  $\text{NiBi}_3$  structural parameters, corresponding to orthorhombic space group  $\text{Pnma}$  (62). In figure 2 is shown the crystalline structure.

Yoshida et al.[14] reported magnetic properties of NiBi. Unlike their samples with important amounts of nickel impurities, our  $\text{NiBi}_3$  samples are completely free of nickel, according to the X- ray diffraction analysis, refinement, and XPS studies as we will show below.

Figure 3 shows SEM - EDS images of  $\text{NiBi}_3$ . A comparison between two of our samples (*a*, *b*) with different reaction times; with three and seven days at  $1000^\circ\text{C}$  are presented, respectively. Sample *a* shows the presence of two phases, NiBi and  $\text{NiBi}_3$ , differentiated by the color

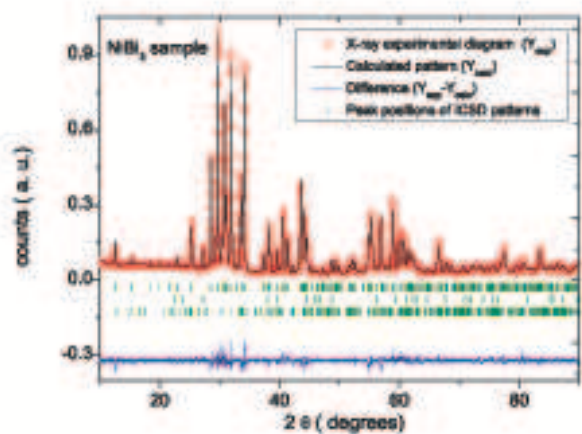


FIG. 1. (Color online) Rietveld refinement of  $\text{NiBi}_3$  sample. Dots are the experimental data, the continuous line superposed to the dots is the calculated pattern. At the bottom of the diagram, the difference between the experimental and calculated points is shown. Vertical marks are displayed in three rows corresponding from top to bottom to the Bragg positions for the phase  $\text{NiBi}_3$ , Bi, and NiBi respectively.

TABLE I. Crystallographic data for  $\text{NiBi}_3$  obtained by Rietveld refinement starting with the structural parameters reported by Fjellvag and Furuseth [15] with symmetry described by the orthorhombic space group  $\text{Pnma}$ . The standard deviations are written between parentheses.

Rp(%)	Rwp(%)	Re(%)	$\chi^2$ [16]
14.0	15.3	11.1	1.886
Parameters ( $\text{\AA}$ )	a = 8.879(1) b = 4.0998(7) c = 11.483(2)		
Volume ( $\text{\AA}^3$ )	417.7(2)		
site	x	y	z
Bi 1	0.298(3)	0.25	0.890(2)
Bi 2	0.382(4)	0.25	0.594(2)
Bi 3	0.409(3)	0.25	0.180(2)
Ni 1	0.09(1)	0.25	0.520(6)

and borders clearly defined. Sample *b* shows a homogeneous composition of  $\text{NiBi}_3$ . Impurities of NiBi and Bi were not detected by EDS.

In order to discard nickel impurities, XPS analysis was performed in our samples. Figure 4a shows the survey spectra for  $\text{NiBi}_3$ . It was observed that all peaks correspond to Ni and Bi, any trace of other elements were found. Figure 4b shows the XPS spectra at low binding energies for the  $\text{NiBi}_3$  sample and its comparison with

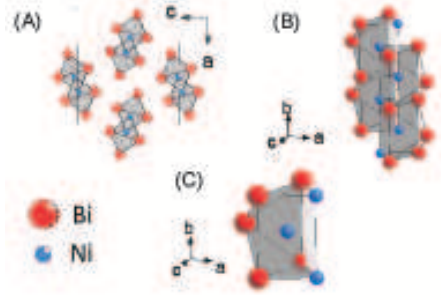


FIG. 2. (Color online) NiBi<sub>3</sub> crystalline structure. (A) Unit cell; (B) Rods of prisms oriented along the b axis; (C) Ni atoms with capped trigonal prismatic coordination and strong bonds Ni-Bi and Ni-Ni.

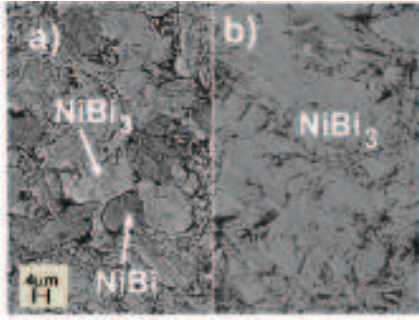


FIG. 3. SEM Images of NiBi<sub>3</sub>. a) NiBi<sub>3</sub> after heating at 1000 °C during 3 days, b) and during 7 days.

bismuth and nickel metal references. The analysis of the sample in the valence region shows that the 3d peak of nickel spectrum displays a increasing width and movement to higher energies with respect to nickel metal. This effect is attributed to changes in the environment of the nickel atoms when forming part of the alloy, confirming that nickel atoms are part of the NiBi<sub>3</sub> compound and not as an impurity.

## B. Superconductivity

Magnetization measurements  $M(T)$  performed in ZFC and FC modes were performed in order to determine the amount of superconducting fraction. The Meissner fraction of NiBi<sub>3</sub> sample was determined to be about 54.1% and was calculated a 2 K related to the maximum value  $-4\pi\chi = -4\pi\rho M/mB$ , where  $\rho$  is the density of the material equal to 10.884 g/cm<sup>3</sup>,  $M$  is the magnetization in emu,  $m$  is the mass in g, and  $B$  is the applied magnetic field [17]. The superconducting transition temperature  $T_C$  was 4.05 K and is defined as the point in which there

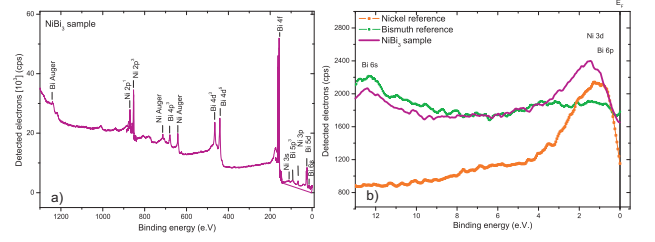


FIG. 4. (Color online) XPS analysis of NiBi<sub>3</sub>. a). XPS survey spectra for NiBi<sub>3</sub>. b). XPS valence band spectra for Ni, Bi, and NiBi<sub>3</sub>. This XPS analysis shows that the compound is a phase without Ni impurities.

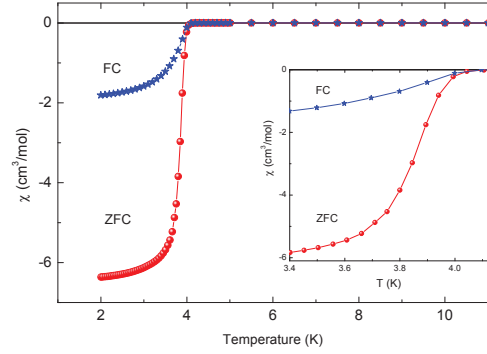


FIG. 5. (Color online) Shielding and Meissner fractions measured at 10 Oe. The inset displays the measurements close to the transition temperature. The onset of the transition is about 4.05 K

is a drop in the susceptibility in the FC measurement. These results are shown in the Fig. 5.

## C. Magnetic measurements.

Magnetization measurements as a function of applied magnetic field  $M(H)$ , were used to calculate the superconducting parameters. The critical magnetic fields  $H_{C1}(0)$  and  $H_{C2}(0)$  were calculated from the experimental data and a linear fit using the expression  $H_{Ci}(0) = -0.693T_C(dH_{Ci}(T)/dT|_{T=T_C})$  near  $T_C$ , where  $dH_{Ci}(T)/dT|_{T=T_C}$  corresponds to the slope of the linear fit [18]. Figure 6 shows the critical magnetic fields.

The Ginzburg-Landau (GL) parameters; coherence length  $\xi_{GL}$ , penetration length  $\lambda_{GL}$ ,  $\kappa$ , and the thermodynamical critical field  $H_C(0)$ , were estimated with the equations:  $H_{C2}(0) = \phi_0/2\pi\xi_{GL}^2$ ,  $H_{C2}(0)/H_{C1}(0) = 2\kappa^2/\ln\kappa$ ,  $\kappa = \lambda_{GL}/\xi_{GL}$ , and

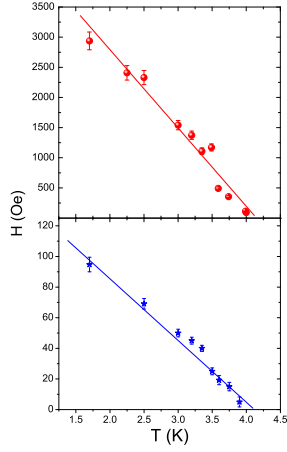


FIG. 6. (Color online) Critical fields  $H_{C1}$ , and  $H_{C2}$  as function of temperature. Critical fields were measured using isothermal magnetic curves, data were fit with the expressions mentioned in the main text.

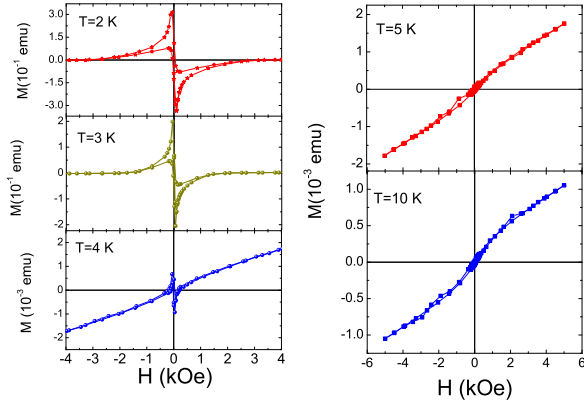


FIG. 7. (Color online) Isothermal magnetic measurements  $M$ - $H$  in the superconducting region of  $\text{NiBi}_3$ , note the anomalous characteristics of data, which is the effect of ferromagnetism in the sample.

$H_C(0) = \phi_0 / (2\sqrt{2}\pi\xi_{GL}\lambda_{GL})$  where  $\phi_0$  is the quantum flux. Also we may use  $H_{C1}H_{C2} = H_C \ln \kappa$ . The superconducting parameters are presented in table II and are similar to the obtained by Fujimori, et al. [13].

#### D. Magnetic measurements below and above $T_C$

As was mentioned before different magnetic measurements were performed to have a better insight about the electronic properties of this alloy. Below the transition

TABLE II. Superconducting parameters of  $\text{NiBi}_3$  compound

Property	Value
$T_C$	$4.05 \pm 0.1$ K
$dH_{C1}(T)/dT _{T=T_C}$	$40 \pm 3$ Oe/K
$dH_{C2}(T)/dT _{T=T_C}$	$1290 \pm 80$ Oe/K
$H_{C1}(0)$	$110 \pm 8$ Oe
$H_{C2}(0)$	$3620 \pm 300$ Oe
$\xi_{GL}$	$302 \pm 10$ Å
$\lambda_{GL}$	$1549 \pm 100$ Å
$\kappa$	$5.1 \pm 0.2$
$H_C(0)$	$490 \pm 30$ Oe

temperature  $M(H)$  measurements were used to determine the critical fields in the usual manner; thus fitting a straight line to the  $M(H)$  curve at different temperatures. Below  $T_C$  at the temperatures of 2, 3, and 4 K, Fig. 7 displays the competition between the diamagnetic characteristic of the superconducting state and the ferromagnetism of the compound. At low field  $M(H)$  curves look normal, so  $H_{C1}$  can be determined. However as soon as the maximum diamagnetism is reached, a fast decrease of the diamagnetic contribution,  $-M$  is observed. This decreasing characteristic changes more rapidly than in normal superconductors (where the magnetism is absent). This anomalous behavior is the indication of two competing processes: superconductivity and ferromagnetism. At high temperature above the transition temperature, where the diamagnetic characteristic disappears,  $M(H)$  shows a typically ferromagnetic characteristic; thus a tendency to saturation of the magnetization at high fields and a coercive field,  $h_C$ , at the central part of the curve.

$M(H)$  measurements were performed in order to determine the coercive field  $h_C$ . We used a medium field model above the superconducting temperature given by:  $h_C(T) = h_C(0)[1 - (T/\tau_C)^{1/2}]$ , in this equation  $\tau_C$  is the Curie temperature. In Fig. 8 we present the variations of  $h_C$  up to 750 K. The fitting line is the result of the above equation for  $h_C$ . At this high temperature we observed in the inset the  $M(H)$  data obtained at 750 K. This last measurement is above the Curie temperature of  $\text{Ni}$   $355^\circ\text{C}$  ( or 627 K [19]). The measurement performed at 750 K clearly indicates that  $\text{NiBi}_3$  is the only magnetic

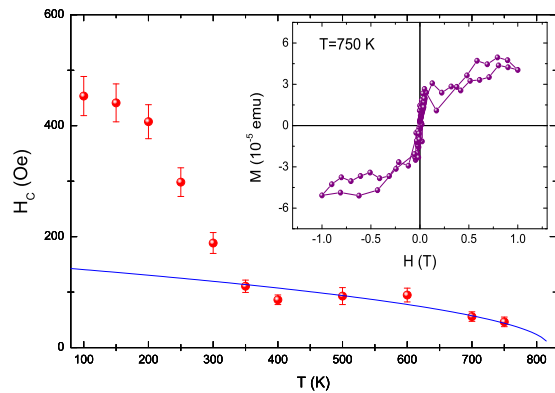


FIG. 8. (Color online) Coercive field extracted from M-H measurements from 100 to 750 K. Clearly the ferromagnetic behavior is observed, and also the coercive field. Accordingly the ferromagnetic transition is above 800 K, and consequently the only magnetic contribution is of NiBi<sub>3</sub>. The inset shows the isothermal measurements at 750 K. At that temperature the ferromagnetic characteristic is still clearly observed at low fields.

contributing material. In the Yoshida's studies they observed that NiBi is magnetic at a maximum about 640 K. Our measurements show that at 750 K the coercive field is small and about 70 Oe.

#### IV. CONCLUSIONS

We found that NiBi<sub>3</sub> is a type II superconducting material in which ferromagnetism and superconductivity coexist and presents an interesting interplay. This is the first time that such coexistence is demonstrated in a clear experimental manner. The ferromagnetic transition is persistent at very high temperature about 750 K, well above the Curie temperature of Ni metal and NiBi compound.

#### ACKNOWLEDGMENTS

We thank F. Silvar for Helium provisions, Lazaro Huerta for the XPS measurements, Francisco M. Ascencio for his collaboration in the sample preparation.

- 
- [1] Ginzburg V. L., *Sov. Phys., JETP*, **4**, 153 (1957)
  - [2] Matthias B., Suhl H. and Corenzwit E., *Phys. Rev. Lett.*, **1**, 449 (1958).
  - [3] Khan, H. R., Raub, C. J., *Ann. Rev. Mater. Sci.*, **15**, 211 (1985).
  - [4] Sinha, K, Kakani, S.L., *Magnetic superconductors. Recent developments*, Nova Science Publisher, inc., New York,(1989).
  - [5] Kakani, S. L., Upadhyaya, U. N., *J. Low Temp. Phys.*, **70**, 5 (1988).
  - [6] Ishikawa, M., Fischer, A. L., *Solid State Commun.*, **23**, 37 (1977)
  - [7] Hamakar, H. C., et al., *Solid State Commun.*, **31**, 139 (1979)
  - [8] Maple, M. B., *Physics Today*, **39**, 72 (1986).
  - [9] Steglich, F., et al., *Phys. Rev. Lett.*, **43**, 1892 (1979)
  - [10] G. P. Vassilev, X. J. Liu, K. Ishida, *J. Phase Equil. Diff.* **26**, 161 (2005)
  - [11] S. Park, K. Kang, W. Hana, T. Vogt, *J. Alloys Compd.* **400**, 88 (2005)
  - [12] N. E. Alekseevskii, N. B. Brandt, and T. I. Kostina: *Bull. Acad. Sci. URSS.* **16**(1952) 233; *J. Exp. Theor. Phys.* **21**, 951 (1951)
  - [13] Fujimori Y, Kan Sh-i, Shinozaki B, Kawaguti T., *J. Phys. Soc. Jpn.*, **69**, 3017 (2000), and references there in.
  - [14] Yoshida H., et al., *Magn. Magn. Mater.*, **239**, 5 (2002).
  - [15] Fjellvag H, Furuseth S, *J. Less-Comm. Met.* **128**, 177 (1987).
  - [16] Young, R. A., *The Rietveld Method*, International Union of Crystallography, Oxford University Press, New York (1993).
  - [17] Lai C. C., Lin T. Y., *Chin. J. Phys.*, **28**, 4 (1990).
  - [18] Li L. F., et al., *Physica C*, **470**, 313 (2010).
  - [19] Kittel, C., *Introduction to Solid State Physics*, 6<sup>th</sup> ed., John Wiley & Sons, inc., New York (1993).